



New Bioactive Sesquiterpenoids From the Plant Endophytic Fungus *Pestalotiopsis theae*

Gaoran Liu^{1,2†}, Ruiyun Huo^{1,2†}, Yanan Zhai¹ and Ling Liu^{1,2*}

¹ State Key Laboratory of Mycology, Institute of Microbiology, Chinese Academy of Sciences, Beijing, China, ² College of Life Sciences, University of Chinese Academy of Sciences, Beijing, China

OPEN ACCESS

Edited by:

Junying Ma,
Chinese Academy of Sciences, China

Reviewed by:

Dewu Zhang,
Chinese Academy of Medical
Sciences, China
Debdulal Banerjee,
Vidyasagar University, India

*Correspondence:

Ling Liu
liul@im.ac.cn

[†] These authors have contributed
equally to this work and share first
authorship

Specialty section:

This article was submitted to
Antimicrobials, Resistance
and Chemotherapy,
a section of the journal
Frontiers in Microbiology

Received: 14 December 2020

Accepted: 09 March 2021

Published: 31 March 2021

Citation:

Liu G, Huo R, Zhai Y and Liu L
(2021) New Bioactive
Sesquiterpenoids From the Plant
Endophytic Fungus *Pestalotiopsis*
theae. *Front. Microbiol.* 12:641504.
doi: 10.3389/fmicb.2021.641504

Three new secondary metabolites pestalotheniins A–C (**1–3**), including two new humulane-derived sesquiterpenoids (**1** and **2**) and one new caryophyllene-derived sesquiterpenoid (**3**), together with five known compounds (**4–8**) were isolated from the crude extract of the plant endophytic fungus *Pestalotiopsis theae* (N635). Their structures were elucidated by the extensive analyses of HRESIMS and NMR spectroscopic data. The absolute configurations of **1–3** were determined by comparison of experimental and calculated electronic circular dichroism (ECD) spectra. The cytotoxic effects of these compounds were evaluated *in vitro*. Compound **6** showed moderate cytotoxicity against T24 and MCF7 cell lines. In addition, compounds **1–8** were also evaluated for antibacterial activity.

Keywords: secondary metabolites, endophytic fungi, sesquiterpenoids, electronic circular dichroism, bioactivity, *Pestalotiopsis theae*

INTRODUCTION

Sesquiterpenoids are a group of naturally occurring 15-carbon isoprenoids, showing diverse structural features and interesting bioactivities (Fraga, 2011, 2013). Humulane-type sesquiterpenoids represent an uncommon type of compound possessing a characteristic 11-membered ring in the molecule, which display a wide range of bioactivities including antibacterial, antifungal, cytotoxic, and immunosuppressive activities (Pulici et al., 1996a; Toyota et al., 2004; Luo et al., 2006; Liao et al., 2013; Chen et al., 2014; Wang et al., 2017; Kapustina et al., 2020). Caryophyllene-derived sesquiterpenoids are a group of structurally unique compounds characterized by the presence of a bicyclo[2.7.0]undecane skeleton, which are believed to be derived from humulane (Ayer and Browne, 1981; Daniewsk et al., 1981). Some caryophyllene derivatives exhibited cytotoxic, immunosuppressive, analgesic, and antimicrobial activities (Collado et al., 1994; Pulici et al., 1996b; Fidy et al., 2016). To date, different humulane-type and caryophyllene-derived sesquiterpenoids have been found in plants (Ghalib et al., 2012; Liao et al., 2013), liverworts (Bardón et al., 1999; Toyota et al., 2004), and fungi (Chen et al., 2014; Guo et al., 2020b). In recent years, these two types of sesquiterpenoids have attracted increasing attention and have become the challenging targets of total synthesis (Takao et al., 2008, 2009).

Fungi have contributed significantly to drug discovery as major sources of lead compounds with inspiring novel structures (Jiang et al., 2018; Wu et al., 2018; Han et al., 2019; Liu et al., 2019; Luo et al., 2019). Plant endophytic fungi, the major group of special environmental fungi inhabiting living plants without any negative effects, have been proven to be a rich source of structurally unique and bioactive secondary metabolites (Petrini et al., 1992; Strobel, 2003;

Strobel et al., 2004). The widely distributed endophytic fungi, *Pestalotiopsis* spp., has attracted much attention owing to the discovery of structurally diverse and biologically active secondary metabolites (Liu et al., 2009, 2010). Some caryophyllene type sesquiterpenoids, such as pestaloporinates A–G and pestaloporonins A–C, have also been reported from *Pestalotiopsis* (Hwang et al., 2015; Liu et al., 2016b). In our search for new bioactive secondary metabolites from this fungal genus, a strain of *P. theae* (N635), isolated from the branches of the tea plant *Camellia sinensis* (Theaceae) in the suburb of Hangzhou, P. R. China, was grown in different solid-substrate fermentation. Chemical studies of the resulting crude extracts had afforded two cytotoxic spiroketals and their putative biosynthetic precursors (Liu et al., 2016a), nine cytotoxic and antioxidant polyketides (Guo et al., 2020a), and five cytotoxic caryophyllene-derived sesquiterpenoids with 4/6/5 ring system (Guo et al., 2020b). Further chemical investigations of these fractions led to the isolation of two new humulane-derived sesquiterpenoids, pestalotheniins A (1) and B (2), one new caryophyllene-derived sesquiterpenoid pestalothenin C (3), together with five known compounds, 14-acetylhumulane (4) (Liu et al., 2016b), 9,15-Dihydroxy-2,6-humuladiene-5,10-dione (5) (Pulici et al., 1996a), punctaporonin H (6) (Wu et al., 2014), pestalotiopsin E (7) (Xiao et al., 2017), and pestalotiopsin C (8) (Pulici et al., 1997; Figure 1). Here we report the isolation, structure elucidation and biological activities of these compounds.

MATERIALS AND METHODS

General Experimental Procedures

IR data were recorded using a Nicolet IS5 FT-IR spectrophotometer. NMR spectra were recorded on a Bruker Avance spectrometer operating at 400, 500, or 600 MHz with tetramethylsilane as an internal standard. HRESIMS data was obtained using an Agilent Accurate-Mass-Q-TOF LC/MS 6520 instrument. Optical rotation was measured by an Anton Paar MCP 200 Automatic Polarimeter. Silica gel (200–300 mesh, Qingdao Ocean Chemical Co., Ltd., China) and Sephadex LH-20 (Amersham Biosciences) were used for column chromatography (CC). HPLC analysis was performed with the Waters 2489 HPLC system using an octadecylsilyl (ODS) column (Pack, ReproSil-Pur Basic, 250 × 4.6 mm, 5 μm) with a flow rate of 1.0 mL/min. HPLC separation was performed on an Agilent HPLC instrument equipped with a variable-wavelength UV detector using an ODS column (C18, 250 × 9.4 mm, 5 μm) with a flow rate of 2.0 mL/min.

Fungal Material

The fungus *P. theae* has been previously described (Guo et al., 2020a).

Fermentation, Extraction, and Isolation

The plant endophytic fungus *P. theae* was grown on PDA at 25°C for 10 days, then several pieces of agar plugs (about 0.5 × 0.5 × 0.5 cm³) were inoculated into 250 mL Erlenmeyer

flasks containing 50 mL of media (0.4% glucose, 1% malt extract, and 0.4% yeast extract) at room temperature on an orbital shaker at 170 rpm for 5 days to produce the seed culture. Finally, 5.0 mL of the spore inoculums obtained from liquid phase cultivation was added to Erlenmeyer flasks (500 mL) containing 80 g of rice and 120 mL of distilled H₂O and incubated at 25°C for 40 days. The fermented rice material was extracted repeatedly with EtOAc (3 × 4.0 L), and the organic solvent was evaporated to dryness to afford the crude extract (15 g), which was fractionated by silica gel vacuum liquid chromatography (VLC), eluted with a gradient of petroleum ether/EtOAc and EtOAc/MeOH to generate 10 fractions (V1–V10). The fraction V3 (950 mg) eluted with 75% petroleum ether/EtOAc was fractionated on a Sephadex LH-20 column chromatography (CC) eluting with CH₂Cl₂:MeOH (1:1) to furnish five subfractions (V3-S1 to V3-S5), and the subfractions V3-S3 (100 mg) was further purified by RP-HPLC (Agilent Eclipse XDB-C18 250 × 9.4 mm, 5 μm column) to provide 1 (*t_R* 13.8 min, 1.5 mg, 60% MeOH/H₂O for 15 min, 2.0 mL/min), 2 (*t_R* 17.8 min, 2.5 mg, 64% MeOH/H₂O for 34 min, 2.0 mL/min), 7 (*t_R* 33.2 min, 1.5 mg, 64–84% MeOH/H₂O for 40 min, 2.0 mL/min) and 8 (*t_R* 17.2 min, 4.2 mg, 39% CH₃CN/H₂O for 25 min, 2.0 mL/min). The fraction V6 (860 mg) eluted with 40% petroleum ether/EtOAc was separated by normal pressure silica gel CC using petroleum ether/EtOAc gradient elution to generate six subfractions (V6-S1 to V6-S6). The subfraction V6-S4 (96 mg) was further purified by RP-HPLC (40% MeOH/H₂O for 16 min, followed by 58% MeOH/H₂O for 14 min, 2.0 mL/min) to afford 5 (*t_R* 16.6 min, 7.5 mg) and 3 (*t_R* 28.6 min, 13.5 mg). The fraction V9 (780 mg) eluted with 90% petroleum ether/EtOAc was subjected to ODS C-18 CC eluting with MeOH/H₂O to get five subfractions (V9-S1 to V9-S5), and further the subfraction V9-S5 purified by RP-HPLC to provide 4 (*t_R* 12.3 min, 5.2 mg, 45–60% MeOH/H₂O for 30 min, 2.0 mL/min). The fraction V10 (380 mg) eluted with 100% EtOAc was subjected to Sephadex LH-20 CC eluting with MeOH to generate four subfractions (V10-S1 to V10-S4), and further the subfraction V10-S3 was purified by HPLC to provide 6 (*t_R* 31.9 min, 10.0 mg, 43% MeOH/H₂O for 35 min, 2.0 mL/min).

Pestalothenin A (1): yellow powder; [α]_D²⁵ –22.0 (*c* 0.1 MeOH); UV (MeOH) λ_{max} (log ϵ) 237 (2.31) nm; CD (*c* 5.0 × 10^{–3} M, MeOH) λ_{max} ($\Delta\epsilon$) 301 (+ 3.1), 259 (+ 6.9), 226 (–10.9) nm; IR (neat) ν_{max} 3,410, 3,352, 2,927, 2,932, 2,880, 2,742, 1,737, 1,712, 1,682, 1,633, 1,248, 1,031 cm^{–1}; ¹H and ¹³C NMR data (see Table 1); HRESIMS *m/z* 329.1373 [M + Na]⁺ (calcd for C₁₇H₂₂O₅Na, 329.1365).

Pestalothenin B (2): colorless oil; [α]_D²⁵ –40.0 (*c* 0.07 MeOH); UV (MeOH) λ_{max} (log ϵ) 204 (1.48) nm; CD (*c* 5.0 × 10^{–3} M, MeOH) λ_{max} ($\Delta\epsilon$) 329 (+ 0.7), 228 (–2.7) nm; IR (neat) ν_{max} 2,977, 2,935, 2,827, 1,744, 1,720, 1,694, 1,635, 1,230, 1,094 cm^{–1}; ¹H and ¹³C NMR data (see Table 1); HRESIMS *m/z* 375.1882 [M + Na]⁺ (calcd for C₁₉H₂₈O₆Na, 375.1886).

Pestalothenin C (3): colorless oil; [α]_D²⁵ –124.0 (*c* 0.1 MeOH); UV (MeOH) λ_{max} (log ϵ) 205 (2.24), 261 (3.72) nm; CD (*c* 3.3 × 10^{–3} M, MeOH) λ_{max} ($\Delta\epsilon$) 336 (+ 3.7), 267 (–9.0), 209 (+ 6.2) nm; ¹H and ¹³C NMR data (see Table 2); HRESIMS *m/z* 251.1665 [M + H]⁺ (calcd for C₁₅H₂₃O₃, 251.1642).

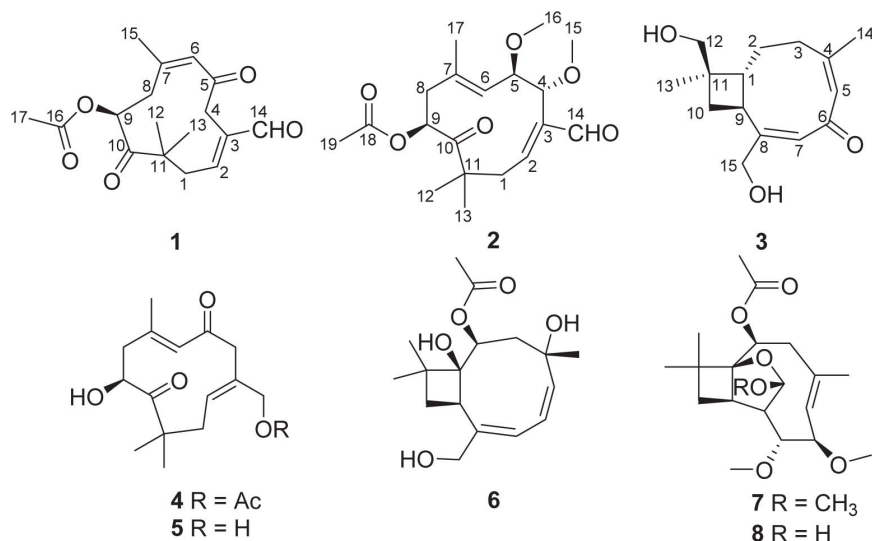


FIGURE 1 | Chemical structures of compounds 1–8.

TABLE 1 | ¹H and ¹³C NMR data of 1 and 2 in CDCl₃.

Position	1 ^a		2 ^b	
	δ _H (J in Hz)	δ _C , type	δ _H (J in Hz)	δ _C , type
1	2.77, dd (16.0, 12.0) 2.16, dd (16.0, 3.0)	40.6, CH ₂	3.38, dd (16.8, 12.0) 1.98, dd (16.8, 3.0)	37.8, CH ₂
2	6.88, dq (12.0, 3.0)	154.2, CH	6.65, dd (12.0, 3.0)	152.3, CH
3		137.2, C		139.3, C
4	3.83, d (15.2) 2.85, dt (15.2, 2.0)	39.4, CH ₂	4.71, d (3.0)	79.2, CH
5		203.3, C	4.14, dd (8.4, 3.0)	78.9, CH
6	5.67, s	128.2, CH	4.73, d (8.4)	128.5, CH
7		149.1, C		134.0, C
8	3.65, dd (15.2, 4.5) 2.37, dd (15.2, 4.5)	31.6, CH ₂	2.85, t (11.5) 2.13, dd (11.5, 3.0)	40.9, CH ₂
9	5.44, t (4.5)	72.1, CH	5.57, dd (11.5, 3.0)	69.3, CH
10		209.5, C		208.3, C
11		47.3, C		47.5, C
12	1.47, s	26.4, CH ₃	1.36, s	26.4, CH ₃
13	1.32, s	25.6, CH ₃	1.35, s	22.1, CH ₃
14	9.47, s	193.2, CH	9.37, s	194.0, CH
15	1.91, s	25.8, CH ₃	3.26, s	57.2, CH ₃
16		170.5, C	3.24, s	56.7, CH ₃
17	2.07, s	20.7, CH ₃	1.86, s	18.2, CH ₃
18				170.0, C
19			2.06, s	21.0, CH ₃

^a¹H (500 MHz) and ¹³C (125 MHz) NMR data in CDCl₃. ^b¹H (600 MHz) and ¹³C (150 MHz) NMR data in CDCl₃.

Computation Section

Systematic conformational analyses were performed via the Molecular Operating Environment (MOE) ver. 2009.10. (Chemical Computing Group, Canada) software package using

the MMFF94 molecular mechanics force field calculation. The MMFF94 conformational analyses were further optimized using DFT at the B3LYP/6-311G(2d,p) basis set level. The stationary points have been checked as the true minima of the potential energy surface by verifying they do not exhibit vibrational imaginary frequencies. The 80 lowest electronic transitions were calculated at the B3LYP/6-311G(2d,p) level, and the rotational strengths of each electronic excitation were given using both dipole length and dipole velocity representations. ECD spectra were stimulated using a Gaussian function with a half-bandwidth of 0.3 eV. Equilibrium populations of conformers at 298.15 K were calculated from their relative free energies (ΔG) using Boltzmann statistics. The overall ECD spectra were then generated according to Boltzmann weighting of each conformer. The systematic errors in the prediction of the wavelength and excited-state energies are compensated for by employing UV correction.

The 3-(4,5-Dimethylthiazol-2-yl)-5-(3-Carboxymethoxyphenyl)-2-(4-Sulfophenyl)-2H-Tetrazolium, Inner Salt (MTS) Assay

In a 96-well plate, each well was plated with (2–5) × 10³ cells (depending on the cell multiplication rate). After cell attachment overnight, the medium was removed, and each well was treated with 100 μL of medium containing 0.1% DMSO, or appropriate concentrations of the test compounds and the positive control cisplatin (100 mM as stock solution of a compound in DMSO and serial dilutions; the test compounds showed good solubility in DMSO and did not precipitate when added to the cells). The plate was incubated at 37°C for 48 h in a humidified, 5% CO₂ atmosphere. Proliferation was assessed by adding 20 μL of MTS (Promega) to each well in the dark, followed by incubation at 37°C for 90 min. The assay plate was read

TABLE 2 | ^1H (400 MHz) and ^{13}C NMR (100 MHz) data for **3** in methanol- d_4 .

Position	δ_{H} (J in Hz)	δ_{C} , type
1	2.45, dt (11.4, 7.8)	43.0, CH
2	1.71, m 1.56, m	22.8, CH ₂
3	2.86, t (11.4) 2.00, dd (12.0, 2.4)	29.4, CH ₂
4		157.0, C
5	6.12, s	130.8, CH
6		196.3, C
7	6.28, s	125.6, CH
8		159.0, C
9	3.80, q (9.6)	33.4, CH
10	2.10, t (11.2) 1.41, dd (11.2, 8.4)	30.4, CH ₂
11		40.7, C
12	3.29, s	70.6, CH ₂
13	1.02, s	18.7, CH ₃
14	2.03, s	25.8, CH ₃
15	4.52, d (16.5) 4.22, dd (16.5, 2.0)	63.5, CH ₂

at 490 nm using a microplate reader. The assay was run in triplicate.

Antibacterial Assay

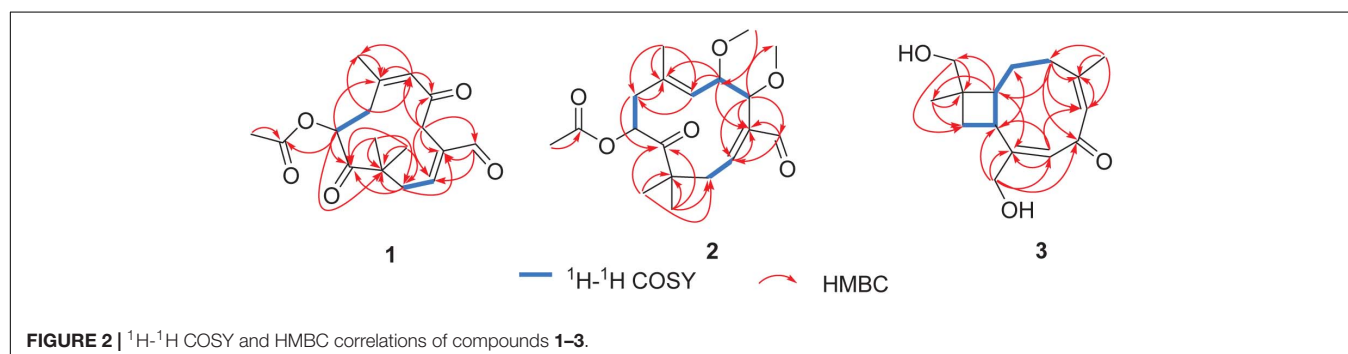
Antibacterial activities of compounds **1–8** were evaluated in replicate as per National Center for Clinical Laboratory Standards recommendations using broth micro dilution method to determine the MIC values with some modifications. In brief, the bacteria were grown in a LB medium (0.5% yeast extract, 1% peptone, 0.5% NaCl in deionized H₂O). The assay was carried out in flat bottom 96-well microtiter plates. Microorganisms were pre-incubated at 37°C for 24 h in medium. Compounds **1–8** were dissolved in DMSO at an initial concentration at 25 mg/mL, and then 1 μL was added to 149 μL medium in 96-well microtiter plates. Then the microorganism solution was added into the 96-well plate (100 μL per well). The densities of the cells were approximately 1.0×10^6 CFU/mL. Positive control drugs were ampicillin (Sigma, purity > 900 $\mu\text{g}/\text{mg}$) for *S. aureus* and *S. pneumoniae*, gentamicin (Sigma, purity \geq 99%) for *E. coli* and *B. subtilis*. After 24 h incubation, the absorbance was determined

at 600 nm by a microplate reader. The MIC value was determined as the lowest concentration inhibiting microbial growth.

RESULTS AND DISCUSSION

Structure Elucidation

Pestalothenin A (**1**) was obtained as a yellow powder. Its molecular formula was established as C₁₇H₂₂O₅ on the basis of HRESIMS spectrum at m/z 329.1373 [M + Na]⁺ (calcd for C₁₇H₂₂O₅Na, 329.1365), indicating 7° of unsaturation. Analysis of the ^1H , ^{13}C (Table 1 and Supplementary Figures 1, 2) and HSQC NMR (Supplementary Figure 4) spectroscopic data of **1** revealed the presence of four singlet methyl groups, three methylenes, one oxymethine, one sp³ quaternary carbon, two trisubstituted olefin units, one carboxylic carbon (δ_{C} 170.5), one aldehyde group (δ_{C} 193.2; δ_{H} 9.47) and two ketone carbons (δ_{C} 203.3 and 209.5, respectively), which accounted for 6° of unsaturation. Therefore, the remaining one unsaturation unit required that compound **1** possessed a monocyclic ring system. In the ^1H - ^1H COSY spectrum (Figure 2 and Supplementary Figure 3), homonuclear vicinal coupling correlations between H₂-1 and H-2 and between H₂-8 and H-9 confirmed the structural fragments of C-1-C-2 and C-8-C-9 in **1**. In the HMBC spectrum (Figure 2 and Supplementary Figure 5), correlations from H-4 to C-2, C-3 and C-14 and from H-14 to C-2, C-3 and C-4 indicated that both C-4 and the aldehyde carbon C-14 (δ_{C} 193.2) were directly connected to the C-2/C-3 olefin at C-3. The HMBC crosspeaks (Figure 2 and Supplementary Figure 5) from H₂-1 to C-11, C-12 and C-13, and from the geminal methyl groups H₃-12 and H₃-13 to C-1, the ketone carbon C-10 (δ_{C} 209.5) and the sp³ quaternary carbon C-11 (δ_{C} 47.3) indicated that C-1, C-10, C-12 and C-13 were all attached to C-11. Furthermore, HMBC correlations (Figure 2 and Supplementary Figure 5) from H₂-8 to C-10 and from H-9 to C-10 and C-11 implied that the ketone carbon C-10 was located between C-9 and C-11. While the cross-peaks from H-9 and H₃-17 to the carboxylic carbon C-16 (δ_{C} 170.5) established the location of the acetyl group at C-9. Other HMBC correlations (Figure 2 and Supplementary Figure 5) from the olefinic proton H-6 to C-5, C-7, C-8 and C-15, from H₂-8 to C-6, C-7 and C-15, and from H₃-15 to C-6, C-7 and C-8 led to the completion of C-5-C-6-C-7-C-8 subunit with the methyl group C-15 attached to the



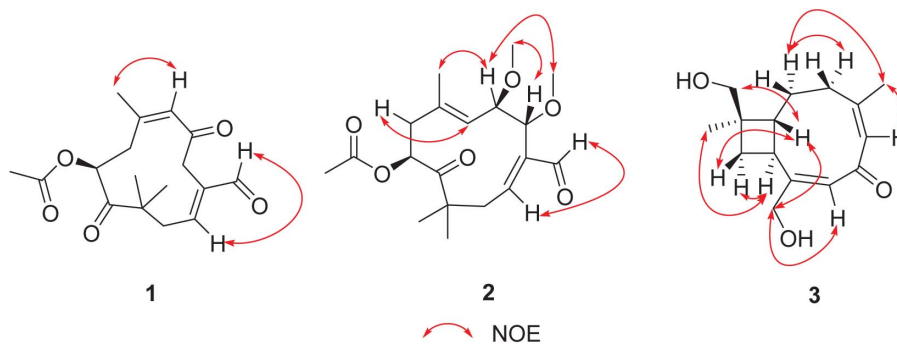


FIGURE 3 | Selected NOESY correlations for compounds **1-3**.

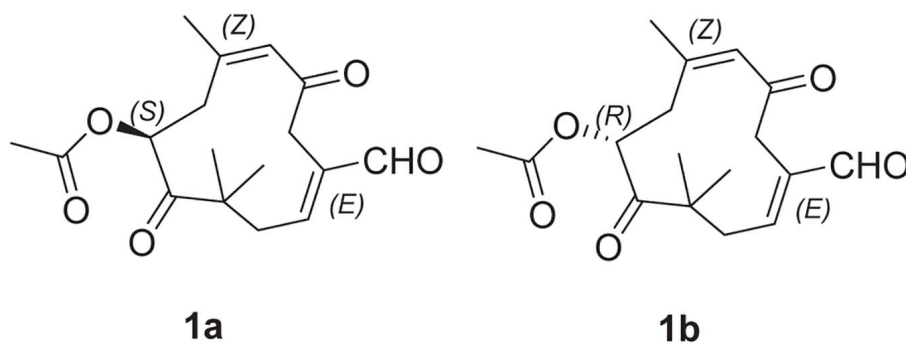
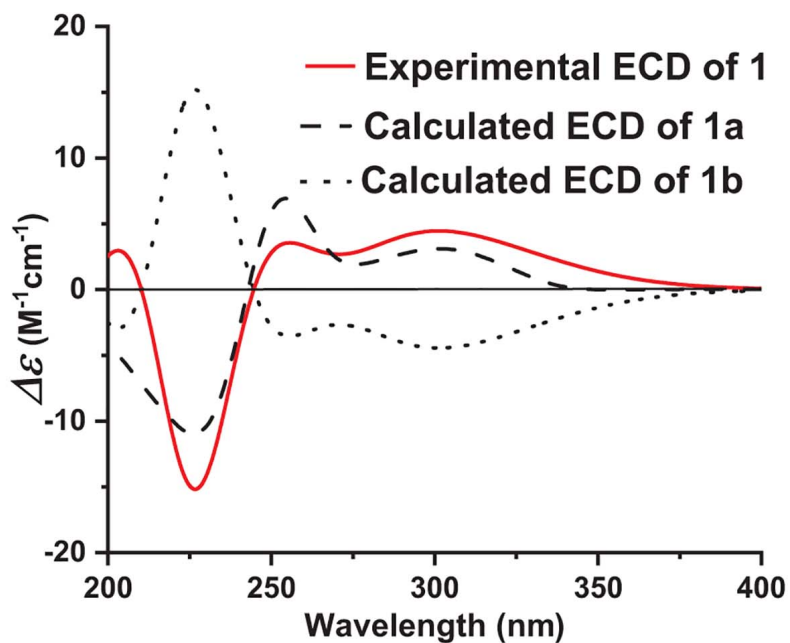
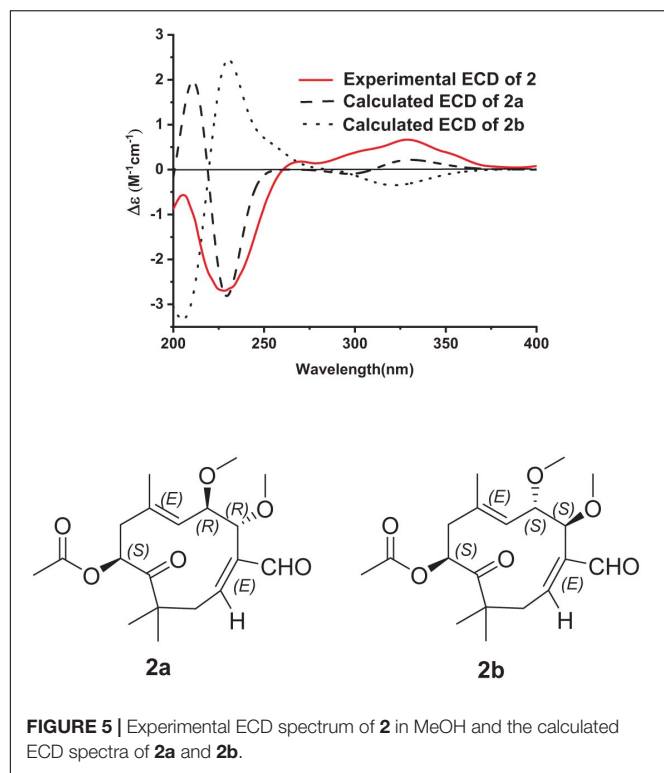


FIGURE 4 | Experimental ECD spectrum of **1** in MeOH and the calculated ECD spectra of **1a** and **1b**.

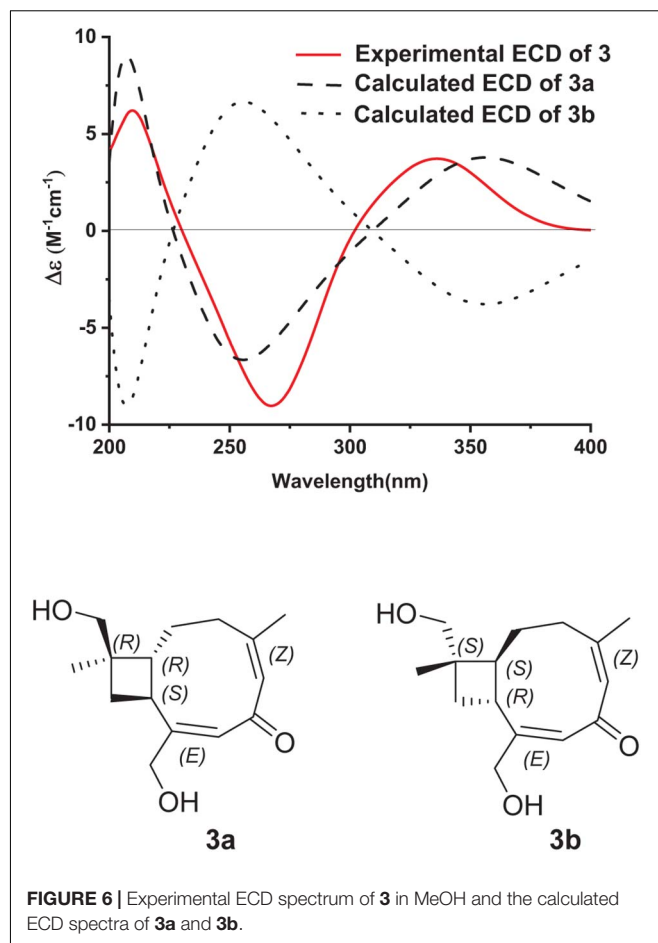
C-6/C-7 olefin at C-7. Key HMBC correlations (**Figure 2** and **Supplementary Figure 5**) from H₂-4 to C-5 and C-6 linked C-4 to the ketone carbon C-6, completing an 11-membered

carbocyclic ring of compound **1**. Thus the planar structure of **1** was determined as a humulane-type sesquiterpenoid as shown. In the NOESY (**Figure 3** and **Supplementary Figure 6**)



spectrum, the cross peak between H-2 and H-14 assigned the C-2/C-3 olefin as *E*-geometry. While the C-6/C-7 olefin of **1** was assigned as *Z*-geometry on the basis of NOESY (**Figure 3** and **Supplementary Figure 6**) correlation of H-6 with H₃-15. To determine the absolute configuration of **1**, a comparison between the experimental and the simulated electronic circular dichroism (ECD) spectra (**Figure 4**) generated by the time-dependent density functional theory (TDDFT) (Zhu et al., 2019) for two enantiomers (9*S*)-**1** (**1a**) and (9*R*)-**1** (**1b**) was performed (**Figure 4**). The MMFF94 conformational search and DFT re-optimization at the B3LYP/6-311G(2d,p) level yielded two lowest energy conformers for **1a** (**Supplementary Figure 19**). The experimental ECD curve of **1** was nearly identical to the calculated ECD spectrum of **1a**, suggested the 9*S* absolute configuration for **1**.

The molecular formula of pestalothenin B (**2**) was deduced as C₁₉H₂₈O₆ (6° of unsaturation) by analysis of HRESIMS spectrum at *m/z* 375.1882 [M + Na]⁺ (calcd for C₁₉H₂₈O₆Na, 375.1886) and NMR data. Analysis of its NMR spectroscopic data (**Table 1** and **Supplementary Figures 7, 8, 10**) revealed the presence of six methyl groups (two methoxy groups), two methylenes, three oxymethines, one sp³ quaternary carbon, two trisubstituted olefin units, one carboxylic carbon (δ_C 170.0), one aldehyde group (δ_C 194.0; δ_H 9.37) and one ketone carbon (δ_C 208.3). These data were similar to those of **1**, indicating that compound **2** was also a humulane-type sesquiterpene. The main differences were that the methylene group at C-4 (δ_{C/H} 39.4/2.85, 3.83) and the ketone carbon C-5 (δ_C 203.3) in **1** were replaced by two oxymethines (δ_{C/H} 79.2/4.71; 78.9/4.14) and two methoxy groups (δ_{C/H} 57.2/3.26; 56.7/3.24) in **2**. These assignments were



further confirmed by 2D NMR data analysis. In the ¹H-¹H COSY spectrum (**Figure 2** and **Supplementary Figure 9**), the cross-peaks of H-4 with H-5 and H-5 with H-6 indicated a C-4-C-5-C-6 subunit of **2**. HMBC correlations (**Figure 2** and **Supplementary Figure 11**) from H-4 to C-2, C-3, C-14 and C-15, from H-5 to C-3, C-7 and C-16, from H₃-15 to C-4 and from H₃-16 to C-5 linked C-4 to C-3 and located two methoxy groups at C-4 and C-5, respectively. Therefore, the planar structure of compound **2** was established as shown. The relative configuration of **2** was assigned by analysis of NOESY data. NOESY correlations (**Figure 3** and **Supplementary Figure 12**) of H-2 with H-14 assigned the C-2/C-3 olefin as *E*-geometry. The C-6/C-7 olefin of **2** was also assigned as *E*-geometry based on NOESY correlations of H-6 with H-8 and H-5 with H₃-17. NOESY correlation (**Figure 3** and **Supplementary Figure 12**) of H-5 with H₃-15 indicated the assignment of the α-configuration of H-5 and H₃-15. While NOESY correlation (**Figure 3** and **Supplementary Figure 12**) of H-4 with H₃-16 indicated that H-4 and H₃-16 were in the β-orientation, thus establishing the relative configuration of **2**. The absolute configuration of C-9 in **2** was deduced as 9*S* on the basis of biosynthetic considerations and by analogy to **1**, **4**, and **5** (Liao et al., 2013; Kapustina et al., 2020). The absolute configurations of C-4 and C-5 in **2** were also deduced by comparison of the experimental and calculated ECD spectra

for the two stereoisomers, (4*R*, 5*R*, 9*S*)-**2** (**2a**) and (4*S*, 5*S*, 9*S*)-**2** (**2b**) (Figure 5). The MMFF94 conformational search and DFT re-optimization at the B3LYP/6-311G(2d,p) level yielded 3 lowest energy conformers for **2a** (Supplementary Figure 19). The overall calculated ECD spectra of **2a** and **2b** were then generated by Boltzmann weighting of the conformers (Figure 5). The experimental CD curve of **2** matched well with the calculated ECD spectrum of **2a**, suggesting that compound **2** has the absolute configuration of 4*R*, 5*R*, 9*S*.

Pestalothenin (**3**) was determined to have the molecular formula C₁₅H₂₂O₃ based on HRESIMS data spectrum at *m/z* 251.1665 [M + H]⁺ (calcd for C₁₅H₂₃O₃, 251.1642) with 5° of unsaturation. Analysis of NMR data (Table 2 and Supplementary Figures 13, 14, 16) of **1** revealed the presence of two methyls, five methylenes (two oxygenated), two methines, one sp³ quaternary carbon, two trisubstituted olefin units, and one α,β-unsaturated ketone carbon (δ_C 196.3). These data accounted for all ¹H and ¹³C resonances except for two exchangeable protons, and suggested that **3** was a bicyclic compound. Analysis of the ¹H-¹H COSY spectrum (Figure 2 and Supplementary Figure 15) of **3** showed one isolated spin-system of C-3-C-2-C-1-C-9-C-10, as shown by the bold bonds in Figure 2. HMBC correlations (Figure 2 and Supplementary Figure 17) from H₂-12 and H₃-13 to C-1, C-10, and C-11, from H-1 and H₂-10 to C-11, C-12 and C-13 allowed the construction of the cyclobutane ring. Further HMBC crosspeaks (Figure 2 and Supplementary Figure 17) from H₂-3 to C-4, C-5, and C-14, from the olefinic proton H-5 to C-3, C-4 and C-14, and from H₃-14 to C-3, C-4 and C-5 indicated that both C-3 and C-14 were directly connected to the C-4/C-5 olefin at C-4. Other correlations (Figure 2 and Supplementary Figure 17) from the olefinic proton H-7 to C-8, C-9 and C-15, from H-9 to C-7, C-8 and C-15, and from H₂-15 to C-7, C-8 and C-9 completed the C-7-C-8-C-9 subunit with C-15 attached to the C-7/C-8 olefin at C-8. Finally, HMBC correlations (Figure 2 and Supplementary Figure 17) from H-5 to C-7, from H-7 to C-5, and from H₂-15 and H-3 to the α,β-unsaturated ketone carbon C-6 (δ_C 196.3) revealed that C-6 was located between C-5 and C-7 to form the cyclononene ring, which was fused to the cyclobutane ring at C-1/C-9 to complete the bicyclo[7.2.0]undeca-2,5-dien-4-one core structure of **3**. The two exchangeable protons were located at C-12 and C-15, respectively, by default, which partially supported by the chemical shift values for C-12 (δ_C 70.6) and C-15 (δ_C 63.5). Thus, the gross structure of **3** was established as a caryophyllene-type sesquiterpenoid (Figure 1). The relative configuration of **3** was established on the basis of the NOESY data (Figure 4). NOESY correlations (Figure 3 and Supplementary Figure 18) of H-5 with H₃-14, and of H-7 with H₂-15 defined the *Z*-geometry and *E*-geometry for C-4/C-5 and C-7/C-8 olefins, respectively. NOESY correlations (Figure 3 and Supplementary Figure 18) of H-1 with H-10, H₂-12 and H₂-15 indicated that these protons were on the same side of the ring system, whereas those of H-9 with H-10 and H₃-13 placed these protons on the opposite side of the molecule, thus establishing the relative configuration of **3**. To establish the absolute configuration of **3**, ECD spectrum of **3** was recorded in MeOH and compared with the DFT-calculated spectra of two enantiomers 1*R*, 9*S*, 11*R* and 1*S*, 9*R*, 11*S* at the B3LYP/6-311 + G(2d,p) level. The

MMFF94 conformational search and DFT re-optimization at the B3LYP/6-311G(2d,p) level yielded 3 lowest energy conformers for **3a** (Supplementary Figure 19). The calculated ECD spectrum of **3a** showed a good agreement with the experimental curve (Figure 6), which supported the absolute configuration being 1*R*, 9*S*, 11*R*. Thus, the completed structure of **3** was elucidated as depicted in Figure 1.

On the basis of the NMR and MS spectroscopic data comparison with those reported in the literatures, in addition to the specific rotation, the other five compounds were identified as 14-acetylhumulane (**4**) (Liu et al., 2016b), 9,15-Dihydroxy-2,6-humuladiene-5,10-dione (**5**) (Pulici et al., 1996a), punctaporonin H (**6**) (Wu et al., 2014), pestalotiopsin E (**7**) (Xiao et al., 2017), and pestalotiopsin C (**8**) (Pulici et al., 1997; Figure 1).

Biological Activity

Compounds **1–8** were evaluated for antibacterial activity against *Staphylococcus aureus* (CGMCC 1.2465), *Bacillus subtilis* (ATCC 6633), *Streptococcus pneumoniae* (CGMCC 1.1692), and *Escherichia coli* (CGMCC 1.2340). However, none of these compounds showed antibacterial activities toward these bacteria (MIC > 50 μg/mL). Compounds **1–8** were tested for cytotoxicity against a panel of five human tumor cell lines, A549 (human lung adenocarcinoma cell line), T24 (human bladder carcinoma cell line), HeLa (human cervical carcinoma cell line), MCF-7 (human breast cancer cell line) and HepG2 (human hepatoma cell line). Compound **6** showed cytotoxic to T24 and MCF-7 cell lines, with IC₅₀ values of 45.7 and 37.6 μM, respectively, whereas the corresponding positive control cisplatin showed IC₅₀ values of 8.4 and 10.5 μM, respectively. While compounds **1–5**, **7**, and **8** did not show detectable inhibitory effects on the cell lines tested at 50 μM.

CONCLUSION

In summary, eight sesquiterpenoids including three new ones, pestalothenins A–C (**1–3**) were identified from the fermentation of the plant endophytic fungus *P. theae* (N635). The structures of the new compounds were elucidated via analyses of their MS, NMR, and ECD spectroscopic data. Pestalothenin A (**1**) differs from the known fungal metabolite 9,15-Dihydroxy-2,6-humuladiene-5,10-dione (**5**) (Pulici et al., 1996a) by different configuration of C-2/C-3 and C-6/C-7 olefins and by having aldehyde and acetyl groups instead of hydroxymethyl and the hydroxy groups at C-3 and C-9, respectively. Pestalothenin B (**2**) is structurally related to pestalothenin A, but differs in having *E*-geometry for C-6/C-7 olefin and having two oxymethines and two methoxy groups rather than the methylene and ketone groups at C-4 and C-5, respectively. Biogenetically, the humulane-type sesquiterpenoids (**1**, **2**, **4**, and **5**) could be derived from humulene which was formed from farnesyl pyrophosphate, first via oxidation, reduction and dehydration, and then followed by a series of methylation and acetylation reactions. While pestalothenin C (**3**) differs from the known humifusane A (Tian et al., 2011) by having oxymethylene group instead of methyl group at C-8. Biogenetically, humulene could be the

biosynthetic mediator of β -caryophyllene which acted as a key precursor in nature to form diverse tricyclic sesquiterpenes by transannular cyclizations. Starting from β -caryophyllene, caryophyllene-type sesquiterpenoids (**3** and **6–8**) could be generated via a series of reactions including transannular cyclization, oxidation, reduction, methylation and acetylation reactions. Compound **6** showed cytotoxic against T24 and MCF-7 cell lines. Our findings not only expand the chemical space of humulane-type and caryophyllene-type sesquiterpenoids, but also suggest that the fungal genus *Pestalotiopsis* might be a rich source of bioactive secondary metabolites.

DATA AVAILABILITY STATEMENT

The datasets presented in this study can be found in online repositories. The names of the repository/repositories and accession number(s) can be found in the article/**Supplementary Material**.

REFERENCES

- Ayer, W. A., and Browne, L. M. (1981). Terpenoid metabolites of mushrooms and related basidiomycetes. *Tetrahedron Lett.* 37, 2199–2248. doi: 10.1016/S0040-4020(01)97979-7
- Bardón, A., Kamiya, N., Toyota, M., Takaoka, S., and Asakawa, Y. (1999). Sesquiterpenoids, hopanoids and bis (bibenzyls) from the Argentine liverwort *Plagiochasma rupestre*. *Phytochemistry* 52, 1323–1329. doi: 10.1016/S0031-9422(99)00452-5
- Chen, Z. M., Fan, Q. Y., Yin, X., Yang, X. Y., Li, Z. H., Feng, T., et al. (2014). Three new humulane sesquiterpenes from cultures of the fungus *Antrodiaella albocinnamomea*. *Nat. Prod. Bioprospect.* 4, 207–211. doi: 10.1007/s13659-014-0032-4
- Collado, I. G., Aleu, J., Macías, S., Antonio, J., and Hernández, G. R. (1994). Inhibition of botrytys cznerea by new sesquiterpenoid compounds obtained from the rearrangement of isocaryophyllene. *J. Nat. Prod.* 57, 738–746. doi: 10.1021/np50108a009
- Daniewsk, W. M., Grieco, P. A., Huffman, J. C., RymkiewLcz, A., and Wawrzun, A. (1981). Isolation of 12-hydroxycaryophyllene-4,5-oxide, a sesquiterpene from *Lactarius camphoratus*. *Phytochemistry* 20, 2733–2734. doi: 10.1016/0031-9422(81)85276-4
- Fidy, K., Fiedorowicz, A., Strzadala, L., and Szumny, A. (2016). β -caryophyllene and β -caryophyllene oxide-natural compounds of anticancer and analgesic properties. *Cancer Med. US* 5, 3007–3017. doi: 10.1002/cam4.816
- Fraga, B. M. (2011). Natural sesquiterpenoids. *Nat. Prod. Rep.* 28, 1580–1610. doi: 10.1039/c1np00046b
- Fraga, B. M. (2013). Natural sesquiterpenoids. *Nat. Prod. Rep.* 30, 1226–1264. doi: 10.1039/c3np70047j
- Ghalib, R. M., Hashim, R., Sulaiman, O., Mehdi, S. H., Valkonen, A., Rissanen, K., et al. (2012). A novel caryophyllene type sesquiterpene lactone from *Asparagus falcatus* (Linn.); Structure elucidation and anti-angiogenic activity on HUVECs. *Eur. J. Med. Chem.* 47, 601–607. doi: 10.1016/j.ejmech.2011.10.037
- Guo, L. F., Lin, J., Niu, S., Liu, S. B., Liu, S. C., and Liu, L. (2020a). Pestalotiones A–D: four new secondary metabolites from the plant endophytic fungus *Pestalotiopsis theae*. *Molecules* 25:470. doi: 10.3390/molecules25030470
- Guo, L. F., Liu, G. R., and Liu, L. (2020b). Caryophyllene-type sesquiterpenoids and α -furanones from the plant endophytic fungus *Pestalotiopsis theae*. *Chin. J. Nat. Med.* 18, 261–267. doi: 10.1016/s1875-5364(20)30032-7
- Han, H., Guo, Z. K., Zhang, B., Zhang, M., Shi, J., Li, W., et al. (2019). Bioactive phenazines from an earwig-associated *Streptomyces* sp. *Chin. J. Nat. Med.* 17, 475–480.
- Hwang, I. H., Swenson, D. C., Gloer, J. B., and Wicklow, D. T. (2015). Pestaloporonins: caryophyllene-derived sesquiterpenoids from a fungicolous isolate of *Pestalotiopsis* sp. *Org. Lett.* 17, 4284–4287. doi: 10.1021/acs.orglett.5b02080
- Jiang, C. S., Zhou, Z. F., Yang, X. H., Lan, L. F., Gu, Y. C., Ye, B. P., et al. (2018). Antibacterial sorbicillin and diketopiperazines from the endogenous fungus *Penicillium* sp. GD6 associated Chinese mangrove *Bruguiera gymnorrhiza*. *Chin. J. Nat. Med.* 16, 358–365. doi: 10.1016/s1875-5364(18)30068-2
- Kapustina, I. I., Makarieva, T. N., Guzii, A. G., Kalinovsky, A. I., Popov, R. S., Dyshlovoy, S. A., et al. (2020). Leptogorgins A–C, Humulane sesquiterpenoids from the vietnamese gorgonian *Leptogorgia* sp. *Mar. Drugs* 18, 310–320. doi: 10.3390/md18060310
- Liao, C. S., Tang, C. P., Yao, S., and Ye, Y. (2013). Humulane-type sesquiterpenoids from *Pilea cavaleriei* subsp. *crenata*. *Org. Biomol. Chem.* 11, 4840–4846. doi: 10.1039/c3ob40872h
- Liu, L., Han, Y., Xiao, J. H., Li, L., Guo, L. D., Jiang, X. J., et al. (2016a). Chlorotheolides A and B, spiroketals generated via Diels–Alder reactions in the endophytic fungus *Pestalotiopsis theae*. *J. Nat. Prod.* 79, 2616–2623. doi: 10.1021/acs.jnatprod.6b00550
- Liu, L., Li, Y., Liu, S. C., Zheng, Z. H., Chen, X. L., Zhang, H., et al. (2009). Chloropestolide A, an antitumor metabolite with an unprecedented spiroketal skeleton from *Pestalotiopsis fici*. *Org. Lett.* 11, 2836–2839. doi: 10.1021/ol901039m
- Liu, L., Niu, S. B., Lu, X. H., Chen, X. L., Zhang, H., Guo, L. D., et al. (2010). Unique metabolites of *Pestalotiopsis fici* suggest a biosynthetic hypothesis involving a Diels–Alder reaction and then mechanistic diversification. *Chem. Comm.* 46, 460–462. doi: 10.1039/b918330b
- Liu, M. T., He, Y., Shen, L., Hu, Z. X., and Zhang, Y. H. (2019). Bipolarins A–H, eight new ophiobolin-type sesterterpenes with antimicrobial activity from fungus *Bipolaris* sp. TJ403-B1. *Chin. J. Nat. Med.* 17, 935–944. doi: 10.1016/s1875-5364(19)30116-5
- Liu, Y., Yang, M. H., Wang, X. B., Li, T. X., and Kong, L. Y. (2016b). Caryophyllene sesquiterpenoids from the endophytic fungus, *Pestalotiopsis* sp. *Fitoterapia* 109, 119–124. doi: 10.1016/j.fitote.2015.12.003
- Luo, D. Q., Gao, Y., Gao, J. M., Wang, F., Yang, X. L., and Liu, J. K. (2006). Humulane-type sesquiterpenoids from the mushroom *Lactarius mitissimus*. *J. Nat. Prod.* 69, 1354–1357. doi: 10.1016/j.bcp.2008.05.019
- Luo, X. W., Lin, Y., Lu, Y. J., Zhou, X. F., and Liu, Y. H. (2019). Peptides and polyketides isolated from the marine sponge-derived fungus *Aspergillus terreus* SCSIO 41008. *Chin. J. Nat. Med.* 17, 149–154.
- Petrini, O., Sieber, T. N., Toti, L., and Viret, O. (1992). Ecology, metabolite production, and substrate utilization in endophytic fungi. *Nat. Toxins* 1, 185–196. doi: 10.1002/nt.2620010306
- Pulici, M., Sugawar, F., Koshino, H., Okada, G., Esumi, Y., Uzawa, J., et al. (1997). Metabolites of *pestalotiopsis* spp., endophytic fungi of

AUTHOR CONTRIBUTIONS

LL designed the experiments. GL and RH performed the experiments. GL, YZ, and LL wrote and revised the manuscript. All authors contributed to the article and approved the submitted version.

FUNDING

This work was supported by and the National Natural Science Foundation of China (32022002, 21772228, and 21977113).

SUPPLEMENTARY MATERIAL

The Supplementary Material for this article can be found online at: <https://www.frontiersin.org/articles/10.3389/fmicb.2021.641504/full#supplementary-material>

- taxus brevifolia*. *Phytochemistry* 46, 313–319. doi: 10.1016/S0031-9422(97)00285-9
- Pulici, M., Sugawara, F., Koshino, H., Uzawa, J., and Yoshida, S. (1996a). Metabolites of endophytic fungi of *Taxus brevifolia*: the first highly functionalized humulane of fungal origin. *J. Chem. Res. Synop.* 8, 378–379. doi: 10.1016/0925-8388(96)02333-X
- Pulici, M., Sugawara, F., Koshino, H., Uzawa, J., and Yoshida, S. (1996b). Pestalotiopsins A and B: new caryophyllenes from an endophytic fungus of *Taxus brevifolia*. *J. Org. Chem.* 61, 2122–2124.
- Strobel, G., Daisy, B., Castillo, U., and Harper, J. (2004). Natural products from endophytic microorganisms. *J. Nat. Prod.* 67, 257–268. doi: 10.1021/np030397v
- Strobel, G. A. (2003). Endophytes as sources of bioactive products. *Microbes Infect.* 5, 535–544. doi: 10.1016/s1286-4579(03)00073-X
- Takao, K. i., Hayakawa, N., Yamada, R., Yamaguchi, T., Morita, U., Kawasaki, S., et al. (2008). Total synthesis of (-)-pestalotiopsin A. *Angew. Chem.* 120, 3474–3477.
- Takao, K. i., Hayakawa, N., Yamada, R., Yamaguchi, T., Saegusa, H., Uchida, M., et al. (2009). Total syntheses of (+)- and (-)-pestalotiopsin A. *J. Org. Chem.* 74, 6452–6461. doi: 10.1021/jo9012546
- Tian, Y., Sun, L. M., Li, B., Liu, X. Q., and Dong, J. X. (2011). New anti-HBV caryophyllane-type sesquiterpenoids from *Euphorbia humifusa* Willd. *Fitoterapia* 82, 251–254. doi: 10.1016/j.fitote.2010.10.005
- Toyota, M., Omatsu, I., Braggins, J., and Asakawa, Y. (2004). New humulane-type sesquiterpenes from the liverworts *Tylimanthus tenellus* and *Marchantia emarginata* subsp. *tosana*. *Chem. Pharm. Bull.* 52, 481–484. doi: 10.1002/chin.200437181
- Wang, J., He, W., Kong, F., Tian, X., Wang, P., Zhou, X., et al. (2017). Ochraceones A-I, humulane-derived sesquiterpenoids from the antarctic fungus *Aspergillus ochraceopetaliformis*. *J. Nat. Prod.* 80, 1725–1733. doi: 10.1021/acs.jnatprod.6b00810
- Wu, Z., Liu, D., Proksch, P., Guo, P., and Lin, W. (2014). Punctaporonins H-M: caryophyllene-type sesquiterpenoids from the sponge-associated fungus *Hansfordia sinuosae*. *Mar. Drugs* 12, 3904–3916. doi: 10.3390/md12073904
- Wu, Z. H., Liu, D., Xu, Y., Chen, J. L., and Lin, W. H. (2018). Antioxidant xanthonones and anthraquinones isolated from a marine-derived fungus *Aspergillus versicolor*. *Chin. J. Nat. Med.* 16, 219–224. doi: 10.1016/s1875-5364(18)30050-5
- Xiao, J., Lin, L. B., Hu, J. Y., Jiao, F. R., Duan, D. Z., Zhang, Q., et al. (2017). Highly oxygenated caryophyllene-type and drimane-type sesquiterpenes from *Pestalotiopsis adusta*, an endophytic fungus of *Sinopodophyllum hexandrum*. *RSC Adv.* 7, 29071–29079. doi: 10.1039/C7RA04267A
- Zhu, S. M., Ren, F. X., Guo, Z., Liu, J. H., Liu, X. Z., Liu, G., et al. (2019). Rogersonins A and B, imidazolone N-Oxide-incorporating indole alkaloids from a *verG* disruption mutant of *Clonostachys rogersoniana*. *J. Nat. Prod.* 82, 462–468. doi: 10.1021/acs.jnatprod.8b00851

Conflict of Interest: The authors declare that the research was conducted in the absence of any commercial or financial relationships that could be construed as a potential conflict of interest.

Copyright © 2021 Liu, Huo, Zhai and Liu. This is an open-access article distributed under the terms of the Creative Commons Attribution License (CC BY). The use, distribution or reproduction in other forums is permitted, provided the original author(s) and the copyright owner(s) are credited and that the original publication in this journal is cited, in accordance with accepted academic practice. No use, distribution or reproduction is permitted which does not comply with these terms.